Nuclear magnetic resonance and unstable rare-earth magnetism in $CeAl_3$

M. J. Lysak and D. E. MacLaughlin
Department of Physics, University of California, Riverside, California 92521
(Received 26 December 1984)

^{27}Al nuclear magnetic resonance (NMR) has been studied in the unstable-moment rare-earth (RE) compound $CeAl_3$ to obtain information on local magnetic behavior. The experiments were carried out at temperatures well above a characteristic temperature $T_{ch} \sim 0.5$ K, below which the system can be described as a degenerate Fermi fluid. A change of slope in the relation between the ^{27}Al isotropic frequency shift K_i and the bulk susceptibility χ is found below ~ 10 K, and is attributed to a temperature-dependent transferred hyperfine field in this temperature range. This hyperfine-field anomaly is probably not the same as that previously noted at $T \simeq T_{ch}$ in other RE compounds ($CeSn_3$, YbCuAl), where the moment instability is associated with intermediate valence. The temperature range is more nearly characteristic of crystalline electric field (CEF) splittings. In $CeAl_2$ an anisotropic hyperfine interaction in the presence of CEF splitting has been invoked to explain a similar shift anomaly. The temperature dependence of the effective Ce-spin fluctuation rate, obtained from measured spin-lattice relaxation rates $1/T_1$, indicates the onset of near-neighbor spatial correlations between dynamic Ce-spin fluctuations at low temperatures, but the nature of these correlations cannot be elucidated from NMR data alone. An effective near-neighbor number $n_{eff} = 7 \pm 2$ is obtained at 300 K. The Korringa product $(K_i^2 T_1 T)_{4f}$ is not strongly enhanced at low temperatures, which is strong evidence against the applicability of a paramagnonlike model to explain the paramagnetism of this compound.

I. INTRODUCTION

The unusual properties of $CeAl_3$ have led to a great deal of experimental and theoretical work on this and related intermetallic compounds.[1] Although the cerium magnetism at high temperatures is well described by a model of independent $Ce^{3+}(^2F_{5/2})$ ions, with full Hund's-rule moments and weak interionic interactions, the properties of $CeAl_3$ at low temperatures are more nearly those of a degenerate Fermi fluid with an extremely low characteristic temperature $T_{ch} \sim 0.5$ K. This gives rise to enormous values of the low-temperature susceptibility[2,3] χ and linear specific-heat coefficient[3] $\gamma = C/T$; the value $\gamma = 1620$ mJ mole^{-1} K^{-2} is the largest yet observed in a metal. The ratio χ/γ, however, is nearly the free-electron value.[3] There is no indication of long-range magnetic order down to 20 mK.[4] Anomalies are also observed in the resistivity,[3] thermopower,[5] thermal expansion,[3,6] magnetoresistance,[2] and elastic properties.[7] Some of these anomalies are observed at temperatures between 10 K and room temperature, and are associated with splitting of the sixfold angular momentum degeneracy of the Ce^{3+} $^2F_{5/2}$ Hund's-rule ground state by crystalline electric fields (CEF). Other anomalies occur near T_{ch}, and are identified with the onset of the low-temperature degenerate Fermi fluid.

In this paper we report the results of ^{27}Al nuclear-magnetic-resonance (NMR) experiments in $CeAl_3$ in the temperature range 1.5–300 K, which were motivated by the unusual behavior noted above. NMR is a *local* probe of magnetism in condensed-matter systems.[8,9] The paramagnetic shift of the NMR resonance frequency for a given applied field is related to the strength of local hyperfine fields at nuclear sites due to electronic moments,[9] and the nuclear spin-lattice relaxation rate yields information on the low-frequency spectrum of thermally-induced electronic spin fluctuations. It is clear at the outset that experiments above 1.5 K will not probe the low-temperature degenerate Fermi-fluid state, but the measurements have yielded information on the effect of CEF splittings and other interactions.

Experimental techniques and results are discussed in Secs. II and III, respectively, and Sec. IV presents a detailed discussion of the results and their implications for the understanding of $CeAl_3$.

II. EXPERIMENTAL TECHNIQUES

A. Sample characterization

$CeAl_3$ crystallizes in the hexagonal Ni_3Sn structure,[10] with lattice constants $a = 6.545$ Å and $c = 4.609$ Å. The space-group designation of this structure is $hP8$ ($P6_3/mmc$), and the point-group symmetries at Ce and Al sites are $\bar{6}m3$ and mm, respectively.[9,10]

Figure 1 shows the structure viewed along the c axis.[11] All Ce atoms are in positions of hexagonal rotation symmetry about the c axis. The numbered arrows in Fig. 1 indicate the near Ce neighbors of an Al site. Each Al site is effectively surrounded by four nearest neighbors at ~ 3.1 Å and 10 next-nearest neighbors at ~ 5.6 Å.

Our experiments were performed on $CeAl_3$ specimens kindly furnished by K. H. J. Buschow, Philips Laboratories, Eindhoven (samples nos. 1 and 2), and by J. Flouquet, Centre de Recherches sur les Très Basses

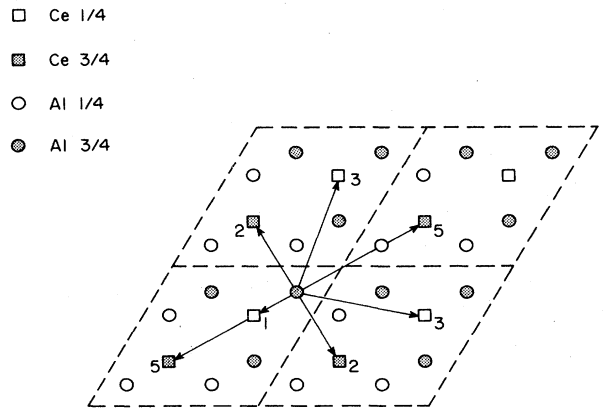

FIG. 1. The Ni_3Sn crystal structure of $CeAl_3$, viewed along the c axis (Ref. 11). The arrows indicate Ce near neighbors of a particular Al site (see text for details).

Températures, Grenoble (sample no. 3), in the form of bulk ingots. To make NMR measurements radio-frequency (rf) field penetration of the sample is necessary. The ingots were therefore powdered and sieved to a grain size $\lesssim 90$ μm, and were not subjected to further heat treatment after powdering.

The phase diagram of the Al-Ce alloy system[9,10] shows that $CeAl_3$ does not form directly from the melt. This gave us cause to investigate the possibility of spurious phases ($CeAl_2$, Ce_3Al_{11}) in our samples. X-ray powder diffraction spectra[12] for our samples could be indexed in the $CeAl_3$ hexagonal structure, with the exception of very small spurious peaks. These corresponded to the $CeAl_2$ structure, with at most a few percent of spurious phase. They were smallest in sample no. 2, which was used for most of the experiments.

B. Measurement techniques

NMR measurements were carried out in external fields between 3.5 and 11 kOe using a pulsed NMR spectrometer.[13] Temperatures between 1.5 and 300 K were obtained using conventional cryogenic techniques. Field-swept absorption spectra were acquired by integrating the spin-echo signal amplitude, followed by averaging using a Nicolet 1170 signal enhancer. The data were then transferred to a Tektronix 4051 computer for analysis. The isotropic NMR shift was obtained from the frequency corresponding to the centroid field of the spectrum.[9] For spectra which were symmetric about a sharp and narrow central peak, the centroid frequency could be found by varying the rf frequency until the free-induction signal, after phase-sensitive detection, was free of "beat" oscillations.

Spin-lattice relaxation times T_1 were measured using standard spin-echo detection of the longitudinal nuclear magnetization recovery after a train of saturating pulses.[13] In most cases the recovery signal exhibited nonexponential behavior, which should not occur for uniform and complete saturation. The observed nonexponentiality may be due either to dipolar cross relaxation,[14] or to multiple-rate relaxation in the presence of quadrupolar splitting of the NMR spectrum.[15] In either case the relaxation data for asymptotically long times approach an exponential time dependence, which yields the correct value of T_1.

III. EXPERIMENTAL RESULTS

A. Field-swept pulsed NMR spectra

Figure 2 shows typical ^{27}Al spectra for the no. 2 sample at a central field of 8 kOe and temperatures of 77, 4.2, and 1.5 K.

At 77 K [Fig. 2(a)] the spectrum is symmetric about the sharp central $(\frac{1}{2}\leftrightarrow-\frac{1}{2})$ transition, and this symmetry is retained for temperatures between 20 and 300 K. The pronounced dip on either side of the central transition is an experimental artifact, which was caused by a combination of interference between free-induction and spin-echo signals and a finite-time window for integration of the echo signal. The satellites of the central transition appear to be quadrupolar in origin. The absence of strong edge singularities in the powder-pattern spectrum at 77 K indicates that the quadrupolar asymmetry parameter η is appreciable[9] which, in turn, makes it difficult to determine

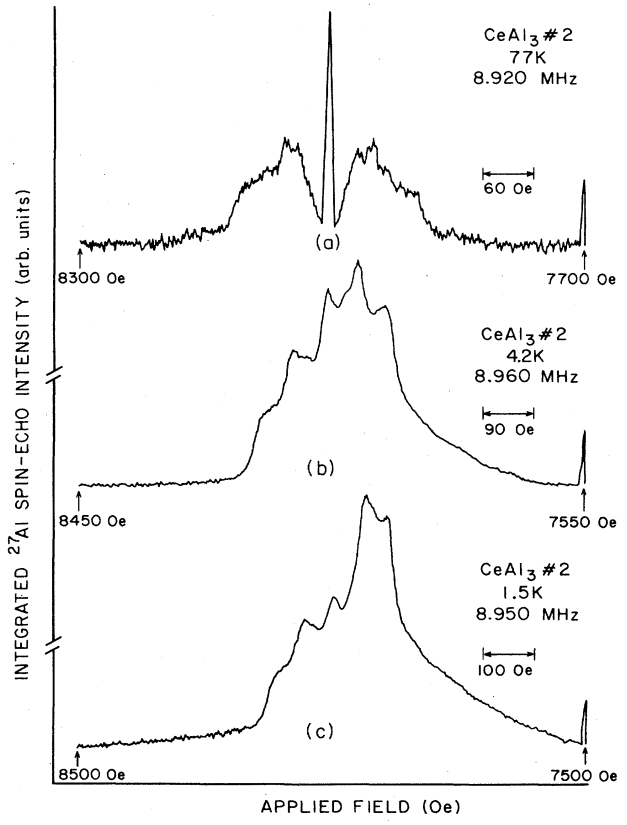

FIG. 2. Field-swept pulsed ^{27}Al spectra of $CeAl_3$ no. 2 at a central field of 8.0 kOe. (a) Temperature $T=77$ K, spectrometer frequency $\nu=8.920$ MHz. (b) $T=4.2$ K, $\nu=8.960$ MHz. (c) $T=1.5$ K, $\nu=8.950$ MHz. The small peak at the low-field end is an experimental artifact.

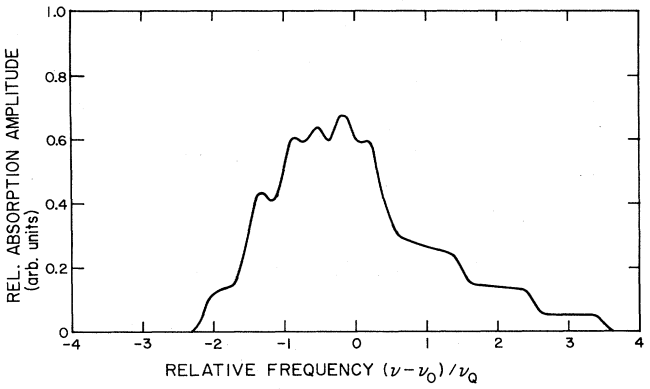

FIG. 3. Calculated first-order NMR powder-pattern spectrum, for comparison with ^{27}Al spectra in $CeAl_3$ at low temperatures (Fig. 2). Frequencies are given in units of the quadrupole splitting ν_Q. For the example given the following parameters were used: nuclear spin $I=\frac{5}{2}$, quadrupole asymmetry parameter $\eta=0.2$, axial anisotropic shift $K_1\nu_0/\nu_Q=1.5$, nonaxial anisotropic shift $K_2\nu_0/\nu_Q=0.4$, Gaussian broadening $\sigma/\nu_Q=0.08$. Here ν_0 is the unshifted Larmor frequency.

the quadrupolar coupling constant e^2qQ/h (or the quadrupolar frequency $\nu_Q=\frac{3}{20}e^2qQ/h$ for $I=\frac{5}{2}$). A crude estimate from Fig. 2(a) yields $\nu_Q\simeq 120(13)$ kHz. Simulated spectra were found to be insensitive to the quadrupole asymmetry, but were consistent with $\eta\geq 0.2$. The shape of the spectrum appears to be temperature independent above ~ 20 K.

Below 20 K the spectra broaden, and an asymmetry in the form of a long tail on the low-field side becomes pronounced. These effects increase with decreasing temperature, as seen in the 4.2 K and 1.5 K spectra of Fig. 2.

Possible distortion of the signal by spurious phases is one potential source of this asymmetry. It could occur either because ^{27}Al nuclei in the spurious phases contribute appreciably to the observed signal, or because the magnetism[16,17] of $CeAl_2$ or Ce_3Al_{11} generates macroscopic dipolar fields at ^{27}Al nuclei in $CeAl_3$. The low fraction of spurious phases from x-ray analysis would seem to rule out the first possibility, whereas the second is unlikely because of the structure which remains in the spectra at low temperatures. Five peaks or shoulderlike features are visible in the spectra of Figs. 2(b) and 2(c), corresponding to the five transitions of a quadrupole-split NMR line for $I=\frac{5}{2}$. Such structures would be washed out in the inhomogeneous field of a macroscopic magnetic inclusion, and we conclude that the broadening is (1) intrinsic, and (2) microscopic in origin.

We therefore consider some of the effects of anisotropy in the NMR shift. If a number of mechanisms contribute to the shift, the mth contribution K_m to the relative shift K is proportional to the product of the mth contribution χ_m to the susceptibility and an associated hyperfine field $H_{\rm hf}^{(m)}$. If either χ_m or $H_{\rm hf}^{(m)}$ are anisotropic, the total shift will possess an anisotropic component K_a.[8,9] Moreover, this anisotropic shift results in an asymmetric spectrum and a broadening proportional to the applied field for a sample in the form of a powder of crystallites. The shape of an anisotropically broadened spectrum can be calculated numerically, and convolution of a Gaussian broadening with the anisotropic powder pattern represents heuristically the effect on the spectrum of dipolar interactions between nuclei.

Figure 3 shows one such simulated spectrum. Although agreement is not perfect, the major features of the experimental $CeAl_3$ spectrum at 4.2 K are reproduced for particular choices of the parameters which govern the quadrupolar splitting and anisotropic shift. We note that the unusual shape of the spectrum is due to the near equality of the anisotropic shift and the quadrupole splitting.

Quantitative measurements of the anisotropic shift are limited in precision to one significant figure by the lack of quantitative agreement between experimental [Fig. 2(b)] and simulated (Fig. 3) spectra. It can be seen, however, that the anisotropic linewidth increases markedly at low temperatures, and has continued to increase with decreasing temperature between 4.2 and 1.5 K. Spectra were obtained from $CeAl_3$ no. 2 at 4.2 K for several fixed frequencies corresponding to field sweeps about central fields between 3 and 11 kOe. The widths of these spectra increase with increasing central field, which is also consistent with attribution of the linewidth to anisotropic shift.

B. Isotropic NMR shift measurements

The two methods used to obtain the isotropic shift K_i have been discussed in Sec. II above. The temperature dependence of K_i thereby obtained is shown in Fig. 4 for $CeAl_3$ no. 2 (open circles). It can be seen that K_i decreases monotonically with increasing temperature between 1.5 and 300 K.

If this temperature dependence is due to temperature-independent transferred hyperfine coupling between ^{27}Al nuclei and the Ce ionic moments, a plot of K_i as a function of the bulk susceptibility χ, with temperature as an implicit parameter, should yield a straight line. Correspondingly, deviations from a linear $K_i(\chi)$ relation are due either to a temperature-dependent hyperfine coupling, caused by temperature variation of the electronic structure involved in the transferred coupling, or to the onset of a new temperature-dependent term in the susceptibility. We have obtained literature values of χ for $CeAl_3$ for several temperature ranges.[3,18–20] The data overlap quite well except for a discrepancy at 10 K of about 9%. The temperature dependence of χ is also given in Fig. 4, with a scale factor chosen for best fit to a linear $K_i(\chi)$ relation at high temperatures as discussed later in this section.

Figure 5 gives K_i versus χ in $CeAl_3$. The solid circles are shift values derived from centroids of the broad low-temperature spectra described above, and the open circles were obtained from free-induction decay signals above ~ 20 K. Following Carter *et al.*,[9] we write a linear relation between K_i and χ as

$$K_i(T)=\frac{H_{\rm hf}}{N\mu_B}\chi(T)+(K_i)_0\,, \tag{1}$$

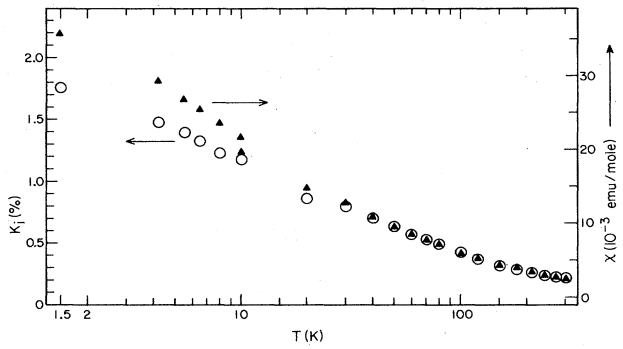

FIG. 4. Temperature dependence of the bulk susceptibility χ (triangles) (Refs. 3 and 18—20) and the ^{27}Al isotropic NMR shift K_i in $CeAl_3$ no. 2. The choice of vertical scales (see text) yields overlap of $\chi(T)$ and $K_i(T)$ at temperatures above $\sim$40 K.

where H_{hf} is the isotropic hyperfine field, N is Avogadro's number, μ_B is the Bohr magneton, and $(K_i)_0$ is the temperature-independent contribution to K_i, due to the conduction-electron Knight shift, orbital shift, etc. It can be seen from Fig. 5 that above 20 K the experimental $K_i(\chi)$ relation is quite linear. A least-squares fit to Eq. (1) was made for $40 \leq T \leq 210$ K, from which we obtain

$$H_{hf} = +3.32(11) \text{ kOe}/\mu_B, \quad (K_i)_0 = +0.064(12)\% .$$

Referring back to Fig. 4, the ordinates for $K_i(T)$ and $\chi(T)$ were scaled using Eq. (1) and the above fit values of H_{hf} and $(K_i)_0$. The high-temperature K_i and χ data overlap to within $\sim$4% from 300 K down to 30 K, where deviation from linearity begins to set in. The discrepancy between literature values of χ at 10 K mentioned above is seen in Figs. 4 and 5 as a discontinuity at this temperature which, fortunately, will not have qualitative significance for the analysis presented below.

C. Spin-lattice relaxation measurements

The experimental spin-lattice relaxation rate $(1/T_1)_{exp}$ is in general a sum of contributions from several relaxation processes. In the case of $CeAl_3$ we may write

$$(1/T_1)_{exp} = (1/T_1)_{4f} + (1/T_1)_{cond} \tag{2}$$

for the experimental ^{27}Al relaxation rate. Here $(1/T_1)_{4f}$ is the contribution of the $4f$ Ce ionic magnetism, and $(1/T_1)_{cond}$ is the relaxation rate due to conduction electrons, often known as Korringa relaxation. This latter contribution must be estimated in order to determine $(1/T_1)_{4f}$.

In the approximation of noninteracting conduction electrons, the Knight shift K and the spin-lattice relaxation time T_1 can be related via the Korringa relation[8,9]

$$K^2 T_1 T = S , \tag{3a}$$

where

$$S \equiv \frac{\hbar}{4\pi k_B} \left[\frac{\gamma_e}{\gamma_n} \right]^2 . \tag{3b}$$

Here γ_e and γ_n are the electronic and nuclear gyromagnetic ratios, respectively. Electron-electron interactions within the conduction band can modify the Korringa relation, which is then usually written as

$$K^2 T_1 T = S/K(\alpha) . \tag{4}$$

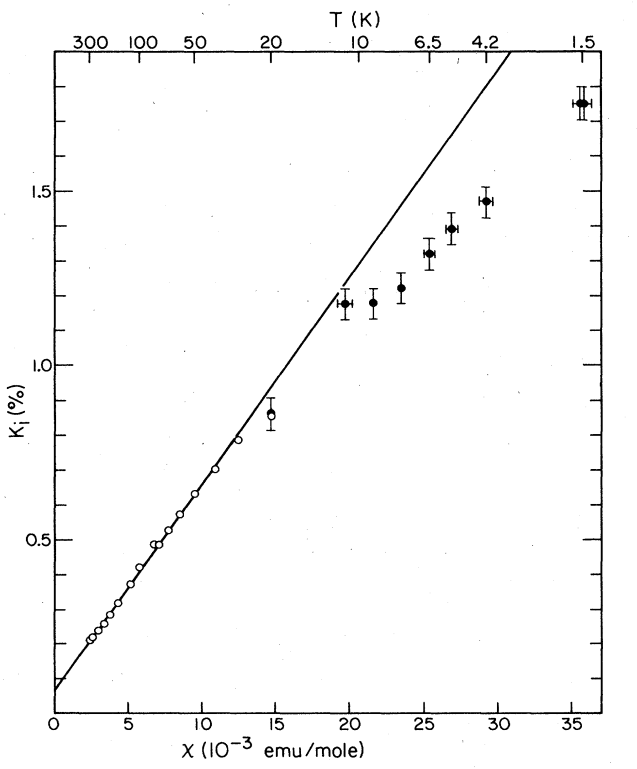

FIG. 5. ^{27}Al NMR shift vs bulk susceptibility χ (Refs. 3 and 18—20), with temperature an implicit variable, in $CeAl_3$. Solid circles: shifts obtained from centroids of field-swept spectra. Open circles: shifts obtained from free-induction resonance frequencies.

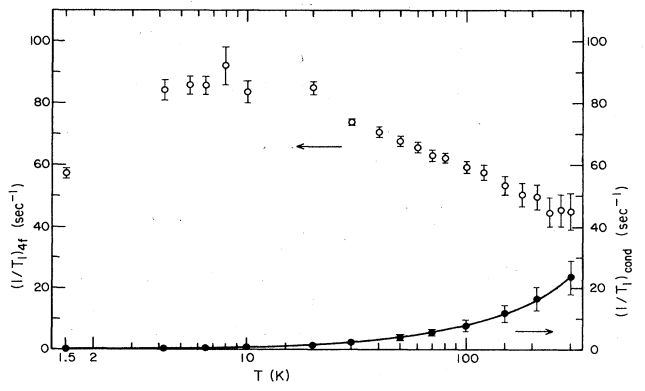

FIG. 6. Temperature dependence of the ^{27}Al spin-lattice relaxation rate in $CeAl_3$ no. 2. Open circles: $4f$ contribution $(1/T_1)_{4f}$. Solid circles and solid curve: estimated contribution to observed $1/T_1(T)$ from *spd*-like conduction electrons [$(T_1T)_{cond} = 13 \pm 3$ sec K]. See text for details.

The Korringa enhancement factor $K(\alpha)$ is related to the strength of the electron-electron interaction, and in general is found to be smaller than unity.

We have used Eq. (4) to estimate the conduction-electron contribution to $(1/T_1)_{\rm exp}$ in $CeAl_3$, with an estimated value of $K(\alpha)$ and the measured value of $(K_i)_0$ obtained from Fig. 5. The estimate of $K(\alpha)$ should in principle be obtained from Knight shift and T_1 measurements in $LaAl_3$, which is a nonmagnetic isomorph of $CeAl_3$ and presumably has a similar conduction-band structure with the exception of $4f$-derived states. Unfortunately no T_1 data have been reported for $LaAl_3$. We use instead shift and relaxation data from a similar compound, $LaAl_2$, for which[9,21]

$$T_1T=14(1)\ \text{sec K},\quad (K_i)_0=+0.06(1)\%\quad (\text{LaAl}_2)\ . \tag{5a}$$

This yields

$$1/K(\alpha)=[(K_i)_0]^2T_1T/S=1.3(4)\quad (\text{LaAl}_2)\ . \tag{5b}$$

Our best estimate for $(1/T_1)_{\rm cond}$ in $CeAl_3$ is thus given by

$$(1/T_1T)_{\rm cond}^{\rm CeAl_3}=K(\alpha)^{\rm LaAl_2}[(K_i)_0^{\rm CeAl_3}]^2/S\ . \tag{6}$$

Finally, from Eqs. (2) and (6) we can estimate the $4f$ contribution $(1/T_1)_{4f}$ to the observed relaxation rate. The temperature dependence of $(1/T_1)_{4f}$ determined in this way is given in Fig. 6, where $(1/T_1)_{\rm cond}$ is also shown for comparison. The latter is not very important below ~ 100 K, which in turn reduces the importance of errors in the above procedure. A broad maximum at $(1/T_1)_{4f}\simeq 85$ sec^{-1} is found near 10 K, with an indication of the beginning of a decrease at 1.5 K. It should be noted that no spin-lattice relaxation can take place in the ground state of any system, so that a marked decrease in $(1/T_1)_{4f}$ must occur between 1.5 K and $T=0$.

IV. DISCUSSION

A. Isotropic NMR shift measurements

A salient feature of our results for the ^{27}Al NMR shift in $CeAl_3$ is the nonlinear behavior of the experimental $K(\chi)$ relation below 20 K (Fig. 5). If a single mechanism controls the temperature dependence of both K and χ, and if the hyperfine field $H_{\rm hf}$ is independent of temperature, then $K(\chi)$ is linear with slope $H_{\rm hf}/(N\mu_B)$. This result is independent of the temperature dependence of χ itself, since the temperature dependence of K is determined only by the temperature-dependent magnetization. The observation of a nonlinear $K(\chi)$ relation then implies either that coupling to a new temperature-dependent magnetization in the system is important, or that the hyperfine field $H_{\rm hf}$ has developed a temperature dependence.[22]

We consider the latter hypothesis first, and treat the temperature dependence of the $4f$ contribution to K_i:

$$(K_i)_{4f}=(K_i)_{\rm exp}-(K_i)_0\ . \tag{7}$$

Together with Eq. (1) this yields for the thermal average $\langle H_{\rm hf}(T)\rangle$ of the hyperfine field

$$\langle H_{\rm hf}(T)\rangle=N\mu_B(K_i)_{4f}/\chi\ , \tag{8}$$

where it is assumed that the observed susceptibility is dominated by the $4f$ contribution; this is the case at low temperatures. Figure 7 gives the temperature dependence of $\langle H_{\rm hf}(T)\rangle$ obtained from this analysis. Temperature-independent values of 2.7 and 3.3 kOe/μ_B are observed at low and high temperatures, respectively, with a point of inflection in the vicinity of 25 K.

We have noted in Sec. I that the characteristic temperature $T_{\rm ch}$ below which degenerate Fermi-fluid behavior and strong correlations are expected to set in is of the order of 0.5 K. The change of slope in the observed $K(\chi)$ relation below ~ 10 K (Fig. 5) is therefore probably not associated with a change in hyperfine interaction at $T_{\rm ch}$. The latter has been observed in some mixed-valent compounds of Ce and Yb,[23] but is weak in the nearly integral-valent compound $CeCu_2Si_2$ (Ref. 24) and absent in nearly integral-valent $CeRu_2Si_2$ (Ref. 25). NMR shift measurements at considerably lower temperatures will obviously be required to determine the situation in $CeAl_3$, but the absence of a NMR shift anomaly at $T_{\rm ch}$ in nearly integral-valent compounds, and at the Kondo temperature T_K for ^{63}Cu satellite NMR shifts[26] in the Kondo alloy *Cu*Fe, lead to the speculation that the anomaly is associated with nonintegral valence rather than Kondo moment instability.[24,25]

Other possible mechanisms for the $K(\chi)$ anomaly involve the splitting of the $(2J+1)$-fold Ce^{3+} degeneracy by the hexagonal crystalline electric field (CEF). Inelastic neutron scattering studies reveal a CEF splitting into three Kramers doublets, with the first excited state separated from the ground state by 50(16) K in the temperature range 100—295 K,[27] and by 60(23) K at a temperature of 5 K.[28] The temperature range below which both the isotropic shift anomaly and the anisotropic shift become large is therefore of the order of these CEF splittings. Similar CEF effects have been observed in the Kondo compound $CeAl_2$,[22] and have been inferred in $CeCu_2Si_2$,[24] although in the latter case the CEF splittings were outside the temperature range of the measurements.

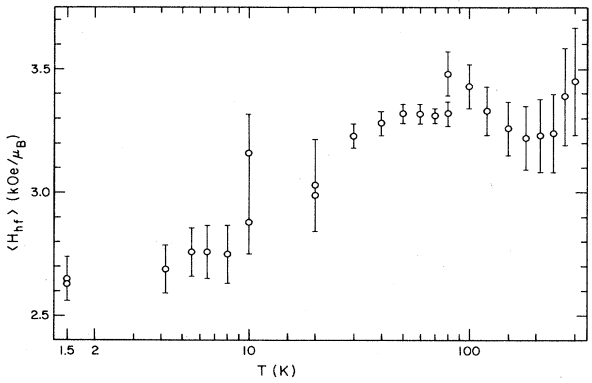

FIG. 7. Temperature dependence of the average ^{27}Al isotropic hyperfine field $\langle H_{\rm hf}\rangle$ in $CeAl_3$ no. 2.

B. Relaxation rate measurements

By an argument similar to that given above for the ^{27}Al NMR shift in $CeAl_3$, it seems unlikely that the temperature dependence of the relaxation rate $1/T_1$ given in Fig. 6 can be due to the onset of a low-temperature degenerate Fermi-fluid state below T_{ch}, at least for data taken above 1.5 K. Two other mechanisms can lead to the observed temperature dependence: (1) dependence of either the hyperfine coupling or the fluctuation rate of the Ce^{3+} moments on CEF state populations,[29] and (2) the onset of short-range correlations in the Ce^{3+} ionic spin fluctuations at low temperatures.[30] The latter, if present, would be sensed by ^{27}Al NMR due to the correlated contribution of local-field fluctuations from Ce^{3+} near neighbors to a given ^{27}Al nucleus.

These two effects can be partially disentangled. A rough argument for the presence of a CEF effect can be made from the fact that the temperature below which both the ^{27}Al $K(\chi)$ anomaly and the shift anisotropy are important, 10 K, is also the temperature at which a broad maximum in $1/T_1(T)$ occurs. We note, however, that temperature dependences due to CEF level populations involve single ions rather than correlations between ions. Now the quasielastic neutron scattering linewidth $\Gamma/2$ measures the lifetime broadening of the CEF ground state, at momentum transfers for which the single-ion magnetic form factor is observed. If single-ion CEF effects dominate, $\Gamma/2$ should have the same temperature dependence as the effective fluctuation rate $1/\tau_{NMR}$ observed by nuclear relaxation.

MacLaughlin *et al.*[22] have discussed extraction of $1/\tau_{NMR}$ from the observed $4f$ contributions to K_i, $1/T_1$, and χ. Values of $1/\tau_{NMR}$, obtained from the expression

$$1/\tau_{NMR}=2N\gamma_n^2 k_B (K_i)^2 T_1 T/\chi \ , \tag{9}$$

are given in Fig. 8, along with the quasielastic neutron scattering linewidth.[31] If Ce-spin fluctuations are uncorrelated, local fields from the several Ce neighbors of ^{27}Al nuclei affect the effective fluctuation rate given by Eq. (9) such that

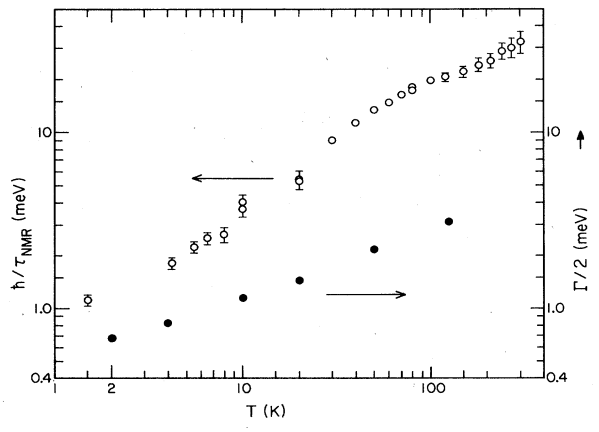

FIG. 8. Estimates of Ce-spin fluctuation rates in $CeAl_3$ from NMR and neutron scattering experiments. Open circles: $\hbar/\tau_{NMR}$ obtained from NMR and bulk susceptibility data. Solid circles: Quasielastic neutron scattering linewidth $\Gamma/2$ (Ref. 29).

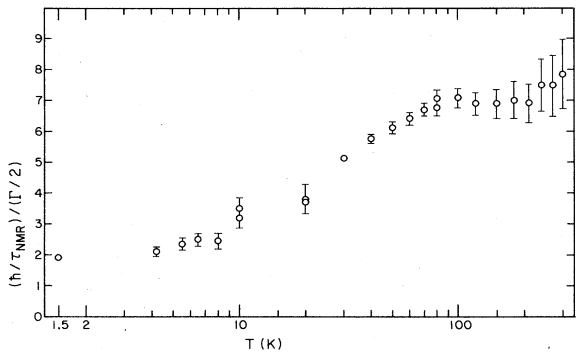

FIG. 9. Temperature dependence of the ratio $(\hbar/\tau_{NMR})/(\Gamma/2)$ from the data of Fig. 8.

$$1/\tau_{NMR}=n_{eff}/\tau \ , \tag{10}$$

where τ is the single-spin correlation time and n_{eff} is an effective number of near-neighbor Ce spins coupled to a given ^{27}Al nucleus. If $\Gamma/2$ is taken to be an experimental determination of $\hbar/\tau$, then the ratio $(\hbar/\tau_{NMR})/(\Gamma/2)$ at high temperatures, where interspin correlations are less likely to be important, yields a measure of n_{eff}. Variation of this ratio with decreasing temperature is then to be taken as an indication of the onset of spatial correlation between Ce-spin fluctuations.[30]

Figure 9 gives the temperature dependence of the ratio $(\hbar/\tau_{NMR})/(\Gamma/2)$ obtained from the data of Fig. 8. The observed value at 300 K is 7(2). This lies between the crystallographic first neighbor and combined first- and second-neighbor coordination numbers of 4 and 14, respectively, and is therefore a reasonable result.[22] At lower temperatures the ratio decreases. This suggests the onset of correlated fluctuations as described above, and therefore indicates that the temperature dependence of $1/\tau_{NMR}$ is not due uniquely to CEF effects. The variation of $(\hbar/\tau_{NMR})/(\Gamma/2)$ is consistent with parallel (ferromagnetic) correlation of ^{27}Al local fields from Ce neighbors. (In the Kondo alloy *Cu*Fe $\hbar/\tau_{NMR}\simeq\Gamma/2$ at temperatures both above and below T_K.[32] Here the ^{63}Cu satellite NMR originates from nuclei coupled to only one Fe spin, and correlations of Fe-spin fluctuations are not observable by NMR.)

C. The Korringa ratio and exchange enhancement

Moriya's theory[33] of the nuclear spin-lattice relaxation rate in exchange-enhanced systems can be applied to the $4f$ relaxation rate itself if, following Béal-Monod and Lawrence,[34] unstable rare-earth magnetism is considered to be due to strong exchange enhancement in a $4f$-derived conduction band. This picture predicts a Curie-Weiss susceptibility above a spin-fluctuation characteristic temperature $T_{ch}=T_{sf}$, as observed in $CeAl_3$, and also predicts for $\chi(T)$ the quadratic temperature dependence with positive coefficient (susceptibility maximum) which is observed for $T\leq T_{sf}$. It is of interest, then, to examine any independent evidence concerning exchange enhancement in unstable-moment rare-earth systems such as $CeAl_3$.

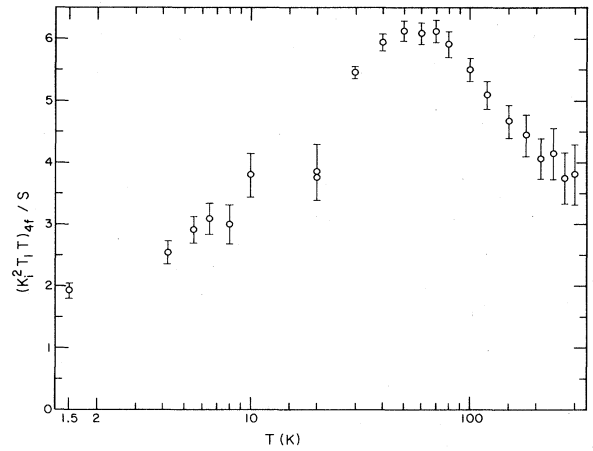

FIG. 10. Temperature dependence of the Korringa ratio $(K_i^2 T_1 T)_{4f}/S$ in $CeAl_3$ no. 2.

In the random-phase approximation (RPA) for spin fluctuations in the conduction band, together with a short-range (δ-function) exchange interaction, the Korringa exchange enhancement factor $K(\alpha)$ can be calculated numerically. In the limit $\alpha \rightarrow 1$ the result can be described as a linear decrease of $K(\alpha)$ to zero: $K(\alpha) \sim 1-\alpha$. Although many approximations are involved in this approach, the basic feature, a decrease of $K(\alpha)$ for $\alpha \rightarrow 1$, should also be found in more complete calculations. One does not expect $K(\alpha)$ to be qualitatively different from $1-\alpha$.

The temperature dependence of the ^{27}Al Korringa ratio $(K_i^2 T_1 T)_{4f}/S$ in $CeAl_3$, obtained from estimates of the Ce $4f$ contributions to K_i and $T_1 T$ obtained above, is given in Fig. 10. It can be seen that this quantity never exceeds a value of about 6, obtained at ~ 60 K, and that it tends to a low-temperature limit of approximately 2. By the argument outlined above this means that within a RPA treatment $K(\alpha)$ is not strongly depressed from unity, particularly at low temperatures, and that the conduction-electron system is therefore not strongly enhanced. This conclusion is consistent with the absence of an enhancement of the low-temperature χ/γ ratio noted in the Introduction, but is novel in that it is based on information obtained from a *local* probe (the ^{27}Al NMR). It is then difficult to understand the enormous low-temperature values of χ and γ as consequences of exchange enhancement, unless the Fermi temperature of the conduction electrons responsible for χ and γ is itself very low. This in turn would require a theoretical explanation.

It is possible, of course, that the nuclear relaxation rate is the sum of contributions from mechanisms other than the isotropic transferred hyperfine interaction, such as the anisotropic hyperfine interaction and dipolar coupling to the relatively well-localized Ce^{3+} $4f$ spin density. These contributions could not, however, decrease $(T_1)_{4f}$ by the 2 to 3 orders of magnitude required to increase our estimate of $K(\alpha)$ to a value consistent with the RPA picture and strong enhancement. We conclude that other mechanisms, such as the Kondo effect or valence mixing, must be considered as origins of the strong heavy-fermion effects in $CeAl_3$.

ACKNOWLEDGMENTS

We are grateful to K. H. J. Buschow and J. Flouquet for providing samples for this investigation, and to numerous co-workers and friends at the Natuurkundig Laboratorium, University of Amsterdam, and the Technische Hochschule, Darmstadt, for discussions of matters related to this work. O. Peña was of immense help in the early stages of the experiments, and the able assistance of S. Stefan is gratefully acknowledged. This research was supported by the U.S. National Science Foundation, Grant No. DMR-8115543, and by the U.C. Riverside Academic Senate Committee on Research.

[1]There are numerous recent reviews of unstable-moment phenomena in rare-earth compounds. See, for example, J. M. Lawrence, P. S. Riseborough, and R. D. Parks, Rep. Prog. Phys. **44**, 1 (1981).

[2]A. S. Edelstein, C. J. Tranchita, O. D. McMasters, and K. A. Gschneidner, Solid State Commun. **15**, 81 (1974).

[3]K. Andres, J. E. Graebner, and H. R. Ott, Phys. Rev. Lett. **35**, 1779 (1975).

[4]A. Benoit, J. X. Boucherle, J. L. Buevoz, J. Flouquet, B. Lambert, J. Palleau, and J. Schweizer, J. Magn. Magn. Mater. **14**, 286 (1979).

[5]P. B. van Aken, H. J. van Daal, and K. H. J. Buschow, Phys. Lett. **49A**, 201 (1974).

[6]M. Ribault, A. Benoit, J. Flouquet, and J. Palleau, J. Phys. (Paris) Lett. **40**, L413 (1979).

[7]M. Niksch, B. Lüthi, and K. Andres, Phys. Rev. B **22**, 5774 (1980).

[8]See, for example, C. P. Slichter, *Principles of Magnetic Resonance* (Harper and Row, New York, 1963).

[9]G. C. Carter, L. H. Bennett, and D. J. Kahan, *Metallic Shifts in NMR* [Prog. Mat. Sci. **20**, 1 (1977)].

[10]J. H. N. van Vucht and K. H. J. Buschow, J. Less-Common Metals **10**, 98 (1965); K. H. J. Buschow and J. H. N. van Vucht, Z. Metallk. **57**, 162 (1966).

[11]K. H. Mader and W. M. Swift, J. Phys. Chem. Solids **29**, 1759 (1968).

[12]We are grateful to O. Peña for obtaining x-ray powder spectra of our samples.

[13]Pulsed NMR techniques are described by I. D. Weisman, L. J. Swartzendruber, and L. H. Bennett, in *Techniques of Metals Research*, edited by E. Passaglia (Wiley, New York, 1973), p. 165.

[14]A. Abragam, *The Principles of Nuclear Magnetism* (Clarendon, Oxford, 1961), Chap. V.

[15]E. R. Andrew and D. P. Tunstall, Proc. Phys. Soc. London **78**, 1 (1961).

[16]B. Barbara, J. X. Boucherle, J. L. Buevoz, M. F. Rossignol, and J. Schweizer, Solid State Commun. **24**, 481 (1977); *ibid.* **29**, 810 (1979).

[17]G. Chouteau, J. Flouquet, J. P. Keradec, J. Palleau, J. Peyrard, and R. Tournier, J. Phys. (Paris) Lett. **39**, L461 (1978).

[18]R. E. Majewski, A. S. Edelstein, and A. E. Dwight, Solid State Commun. **31**, 315 (1979).

[19]A. S. Edelstein, T. O. Brun, G. H. Lander, O. D. McMasters, and K. A. Gschneidner, *Magnetism and Magnetic Materials—1974 (San Francisco),* proceedings of the 20th Annual Conference on Magnetism and Magnetic Materials, edited by C. D. Graham, G. H. Lander, and J. J. Rhyne (AIP, New York, 1975), p. 428.

[20]A. M. van Diepen, H. W. de Wijn, and K. H. J. Buschow, J. Chem. Phys. **46**, 3489 (1967).

[21]M. R. McHenry, B. G. Silbernagel, and J. H. Wernick, Phys. Rev. B **5**, 2958 (1972).

[22]D. E. MacLaughlin, O. Peña, and M. Lysak, Phys. Rev. B **23**, 1039 (1981).

[23]D. E. MacLaughlin, in *Valence Fluctuations in Solids,* edited by L. M. Falicov, W. Hanke, and M. B. Maple (North-Holland, Amsterdam, 1981), p. 321.

[24]J. Aarts, F. R. de Boer, and D. E. MacLaughlin, Physica (Utrecht) **121B**, 162 (1983).

[25]L. C. Gupta, D. E. MacLaughlin, C. Tien, C. Godart, M. A. Edwards, and R. D. Parks, Phys. Rev. B **28**, 3673 (1983).

[26]J. B. Boyce and C. P. Slichter, Phys. Rev. Lett. **32**, 61 (1974); H. Alloul, Physica (Utrecht) **86-88B**, 449 (1977).

[27]P. A. Alekseev, I. P. Sadikov, I. A. Markova, E. M. Savitskii, V. F. Terekhova, and O. D. Chistyakov, Fiz. Tverd. Tela (Leningrad) **18**, 2509 (1976) [Sov. Phys.—Solid State **18**, 1466 (1976)].

[28]A. P. Murani, K. Knorr, and K. H. J. Buschow, in *Crystal Field Effects in Metals and Alloys,* edited by A. Furrer (Plenum, New York, 1977), p. 268.

[29]K. W. Becker, P. Fulde, and J. Keller, Z. Phys. B **28**, 9 (1977).

[30]B. G. Silbernagel, V. Jaccarino, P. Pincus, and J. H. Wernick, Phys. Rev. Lett. **20**, 1091 (1968); E. Dormann, R. D. Hogg, D. Hone, and V. Jaccarino, Physica (Utrecht) **86-88B**, 1183 (1977); R. D. Hogg, Ph.D. thesis, University of California, Santa Barbara, 1975 (unpublished).

[31]A. P. Murani, K. Knorr, K. H. J. Buschow, A. Benoit, and J. Flouquet, Solid State Commun. **36**, 523 (1980).

[32]H. Alloul, J. Phys. (Paris) Lett. **37**, L205 (1976).

[33]T. Moriya, J. Phys. Soc. Jpn. **18**, 516 (1963); see also M. T. Béal-Monod, Phys. Rev. B **28**, 1630 (1983).

[34]M. T. Béal-Monod and J. M. Lawrence, Phys. Rev. B **21**, 5400 (1980).